New Positive-sequence Voltage Detector for Grid Synchronization of Power Converters under Faulty Grid Conditions

P. Rodríguez[⋏], R. Teodorescu[⋆], I. Candela[⋏], A.V. Timbus[⋆], M. Liserre[✱] and F. Blaabjerg[⋆]

[⋏] Technical University of Catalonia
Department of Electrical Engineering
Barcelona – Spain
prodriguez@ee.upc.edu

[⋆] Aalborg University
Institute of Energy Technology
Aalborg – Denmark
ret@iet.aau.dk

[✱] Polytechnic of Bari
Dept. of Electrotechnical and Electronic Eng.
Bari – Italy
liserre@poliba.it

Abstract— This paper deals with a fundamental aspect in the control of grid-connected power converters, i.e., the detection of the positive-sequence component at fundamental frequency of the utility voltage under unbalanced and distorted conditions. Accurate and fast detection of this voltage component under grid faults is essential to keep the control over the power exchange with the grid avoiding to trip the converter protections and allowing the ride-through of the transient fault.

In this paper, the systematic use of well known techniques conducts to a new positive-sequence voltage detection system which exhibits a fast, precise, and frequency-adaptive response under faulty grid conditions. Three fundamental functional blocks make up the proposed detector, these are: *i)* the quadrature-signals generator (QSG), *ii)* the positive-sequence calculator (PSC), and *iii)* the phase-locked loop (PLL). A key innovation of the proposed system is the use of a dual second order generalized integrator (DSOGI) to implement the QSG. For this reason, the proposed positive-sequence detector is called DSOGI-PLL. A detailed study of the DSOGI-PLL and verification by simulation are performed in this paper. From the obtained results, it can be concluded that the DSOGI-PLL is a very suitable technique for characterizing the positive-sequence voltage under grid faults.

I. INTRODUCTION

Grid synchronization is one the most important issues in the integration of power converter into power systems. In particular, this aspect becomes crucial in the connection of wind turbines (WT) to power systems. In recent years, rapid development of WT and increasing penetration of wind power generation have resulted in the reformulation of the grid connection requirements (GCR) for wind power [1]. CGR of the most of the countries with a high rate of wind power penetration state that WT have to ride-through of transient faults to sustain generation. In such grid faults, the amplitude, phase and frequency of the utility voltages can show significant transient variations. Therefore the fast and accurate detection of the positive-sequence component of the utility voltage is necessary in order to keep generation up according to the GCR.

When it is assumed that the frequency of the utility is a constant and well-known magnitude, an algorithm based on the instantaneous symmetrical components (ISC) method can be easily implemented for effective detection of the positive-sequence component [2]. In Europe the frequency is usually 50±0.1 Hz and falls out of the 49-50.3 range very seldom [3]. However, during a transient fault, the system frequency can show significant fluctuations. Regarding the GCR for wind power, the control system of the grid connected converter must ensure its fast adaptation to the faulty conditions, improving the fault tolerance of the wind generation system and avoiding the post-fault collapse of the power system because wind generators are lost.

On the other hand, when the utility frequency is not constant, the positive-sequence detection system uses closed-loop adaptive methods in order to render it insensitive to input frequency variations. The use of a phase-locked loop (PLL) is indeed the most representative example of such frequency adaptive methods. In three-phase systems, the PLL's are usually based on the synchronous reference frame (SRF-PLL) [4]. Under ideal utility conditions, i.e., neither imbalance nor harmonic distortion, the SRF-PLL yields good results. In case the utility voltage is distorted with high-order harmonics, the SRF-PLL can still operate satisfactorily if its bandwidth is reduced in order to reject and cancel out the effect of these harmonics on the output. But under voltage unbalance however, the bandwidth reduction is not an acceptable solution since the overall dynamic performance of the PLL system would become unacceptably deficient [5]. This drawback can be overcome by using a PLL based on the decoupled double synchronous reference frame (DSRF-PLL) [6]. In the DSRF-PLL, a decoupling network permits a proper isolation of the positive- and negative-sequence components. An alternative technique for frequency-adaptive positive-sequence detection is presented in [7]. Such technique uses a single-phase enhanced phase-locked loop (EPLL) for each phase of the three-phase system allowing fundamental frequency adaptation. The phase voltages and its respective 90-degree shifted versions detected by the EPLL are used by the ISC method in order to detect the positive-sequence voltages of the three-phase system. Finally, a fourth single-phase EPLL is applied to the output of the ISC method to estimate the phase-angle of the positive-sequence voltage.

This work presents a new frequency-adaptive positive-sequence detection technique, namely the 'Dual Second Order Generalized Integrator PLL' (DSOGI-PLL). This technique translates the three-phase voltage from the *abc* to the $\alpha\beta$ reference frames. A dual SOGI-based quadrature-signals generator (QSG) is used for filtering and obtaining the 90-degree shifted versions from the $\alpha\beta$ voltages. These signals act as inputs to the positive-sequence calculator (PSC) which lies on the ISC method on the $\alpha\beta$ domain. Finally, the positive-sequence $\alpha\beta$ voltages are translated to the *dq* synchronous reference frame and a PLL (SRF-PLL) is employed to make the system frequency-adaptive.

II. POSITIVE-SEQUENCE CALCULATION ON THE $\alpha\beta$ REFERENCE FRAME

At early 30's, *Lyon* extended the use of the *Fortescue*'s symmetrical components method to the time-domain [8]. Using that principle, the instantaneous positive-sequence component $\mathbf{v}^{+}_{abc}$ of a generic three-phase voltage vector $\mathbf{v}_{abc}=\begin{bmatrix}v_a & v_b & v_c\end{bmatrix}^T$ is given by:

$$\mathbf{v}^{+}_{abc}=\begin{bmatrix}v^{+}_a & v^{+}_b & v^{+}_c\end{bmatrix}^T=\begin{bmatrix}T_+\end{bmatrix}\mathbf{v}_{abc},$$
$$\begin{bmatrix}T_+\end{bmatrix}=\frac{1}{3}\begin{bmatrix}1 & a^2 & a\\ a & 1 & a^2\\ a^2 & a & 1\end{bmatrix},\quad a=e^{-j\frac{2\pi}{3}}. \tag{1}$$

Using the non-normalized *Clarke* transformation, the voltage vector can be translated from the *abc* to the $\alpha\beta$ reference frames as follow:

$$\mathbf{v}_{\alpha\beta}=\begin{bmatrix}v_\alpha & v_\beta\end{bmatrix}^T=\begin{bmatrix}T_{\alpha\beta}\end{bmatrix}\mathbf{v}_{abc},$$
$$\begin{bmatrix}T_{\alpha\beta}\end{bmatrix}=\frac{2}{3}\begin{bmatrix}1 & -\frac{1}{2} & -\frac{1}{2}\\ 0 & \frac{\sqrt{3}}{2} & -\frac{\sqrt{3}}{2}\end{bmatrix}. \tag{2}$$

Therefore, the instantaneous positive-sequence voltage on the $\alpha\beta$ reference frame can be calculated by:

$$\mathbf{v}^{+}_{\alpha\beta}=\begin{bmatrix}T_{\alpha\beta}\end{bmatrix}\mathbf{v}^{+}_{abc}=\begin{bmatrix}T_{\alpha\beta}\end{bmatrix}\begin{bmatrix}T_+\end{bmatrix}\mathbf{v}_{abc}$$
$$=\begin{bmatrix}T_{\alpha\beta}\end{bmatrix}\begin{bmatrix}T_+\end{bmatrix}\begin{bmatrix}T_{\alpha\beta}\end{bmatrix}^{-1}\mathbf{v}_{\alpha\beta}=\frac{1}{2}\begin{bmatrix}1 & -q\\ q & 1\end{bmatrix}\mathbf{v}_{\alpha\beta},\quad q=e^{-j\frac{\pi}{2}}, \tag{3}$$

where q is a phase-shift operator in the time-domain which obtains the quadrature-phase waveform (90-degrees lag) of the original in-phase waveform.

Transformation of (3) is implemented in the PSC of the proposed DSOGI-PLL and its right operation depends on the precision of the quadrature-phase signal provided to its input. It is worth to remark that the time-delay introduced by the q operator is dynamically set according the fundamental frequency of the input voltage. Therefore, the positive-sequence component calculated from the n^{th}-order harmonic at the input voltage is given by:

$$\mathbf{v}^{+}_{\alpha\beta}=\frac{1}{2}\begin{bmatrix}1 & -|n|q\\ |n|q & 1\end{bmatrix}\mathbf{v}^{n}_{\alpha\beta}, \tag{4}$$

where the positive –negative sign of n represents the positive –negative-sequence of the input voltages. From (4), the harmonic rejection capability of the PSC on the $\alpha\beta$ reference frame can be summarized as in Table I, where cells for characteristic harmonics have been highlighted. The PSC does not act as a sequence changer. Consequently, if negative-sequence signals are applied to the PSC input they will arrive to its output with the same sequence but multiplied by the complex factor specified in Table I. In this sense, positive-sequence calculation of (3) is better than that shown in (1) since this second transformation is transparent for characteristic harmonics propagation.

TABLE I

HARMONIC PROPAGATION IN THE PSC ($\mathbf{v}^{+}_{\alpha}$ WHEN $\mathbf{v}^{n}_{\alpha}=1\angle 0^\circ$)

Order	Input signals sequence	
n	+	-
1st	$1\angle 0^\circ$	0
2nd	$1/\sqrt{2}\angle -45^\circ$	$1/\sqrt{2}\angle 45^\circ$
3rd	0	$1\angle 0^\circ$
4th	$1/\sqrt{2}\angle 45^\circ$	$1/\sqrt{2}\angle -45^\circ$
5th	$1\angle 0^\circ$	0
…	…	…

A relevant aspect to be analyzed in the PSC is the error made in the positive-sequence estimation when the frequency setting the time-delay of the q operator, ω', differs from the actual center grid frequency, ω. In such unsynchronized conditions, the complex factor affecting to an n^{th}-order harmonic at the input of the PSC is given by:

$$\mathbf{v}^{+}_{\alpha}=\mathbf{C}^{n}\cdot\mathbf{v}^{n}_{\alpha}\begin{cases}\left|\mathbf{C}^{n}\right|=\sqrt{\frac{1}{2}\left[1+\sin\left(n\frac{\omega}{\omega'}\frac{\pi}{2}\right)\right]}\\ \angle\mathbf{C}^{n}=\operatorname{sgn}(n)\tan^{-1}\dfrac{\cos\left(n\frac{\omega}{\omega'}\frac{\pi}{2}\right)}{2\left|\mathbf{C}^{n}\right|^2}\end{cases} \tag{5}$$

For the sake of clarifying, a numerical example is presented here. In this example, the frequency determining the time-delay of the q operator is $\omega'=50\text{Hz}$ whereas the actual grid frequency is $\omega=40\text{Hz}$. In such conditions, if the components of the grid voltage are $\mathbf{v}^{+1}_{\alpha}=80\angle 0^\circ$, $\mathbf{v}^{-1}_{\alpha}=20\angle -10^\circ$ and $\mathbf{v}^{-5}_{\alpha}=10\angle 30^\circ$, the $\mathbf{v}^{+}_{\alpha}$ voltage at the PSC output is composed by $\mathbf{C}^{+1}\mathbf{v}^{+1}_{\alpha}=79\angle 9^\circ$, $\mathbf{C}^{-1}\mathbf{v}^{-1}_{\alpha}=3.13\angle -91^\circ$, and $\mathbf{C}^{-5}\mathbf{v}^{-5}_{\alpha}=7.07\angle -15^\circ$. The amplitude of $\mathbf{v}^{+}_{\beta}$ is the same that of $\mathbf{v}^{+}_{\alpha}$ but its phase-angle is either 90-degrees lag or lead when the input voltage sequence is either positive or negative, respectively. This numerical example has been illustrated in Fig. 1, where the grid frequency changes from ω=50Hz to ω=40Hz at t=0.15s with ω'=50Hz permanently.

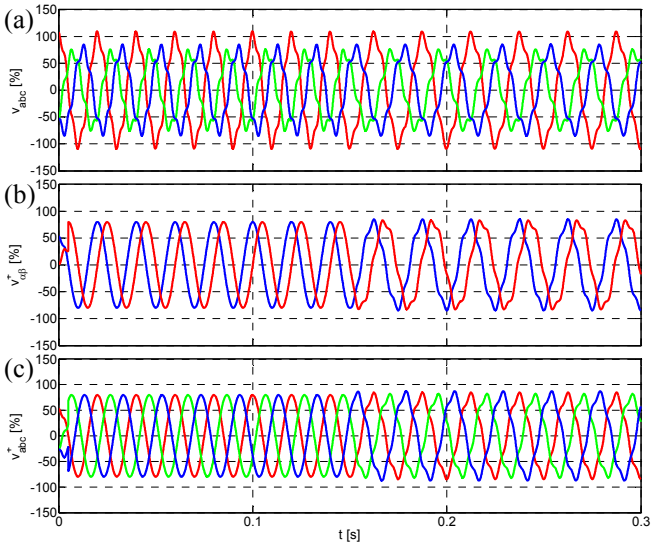

Fig. 1. PSC output when grid frequency changes (ω=40Hz, ω'=50Hz).

III. SECOND ORDER GENERALIZED INTEGRATOR FOR QUADRATURE-SIGNALS GENERATION

A transport delay buffer was used to easily achieve the 90-degrees shifted version of v_α and v_β signals in simulation of Fig. 1. Another simple quadrature-signals generator (QSG) can be implemented by means of a first-order all-pass filter. However, such techniques are not frequency-adaptive, which could give rise to errors in the positive-sequence estimation, e.g. in Fig. 1. Moreover, these simple techniques do not block harmonics from the input signals. To overcome these drawbacks, the use of a single-phase EPLL is proposed in [7]. The EPLL is actually an adaptive notch-filter based on minimizing the product of quadrature-signals [9] and whose frequency moves based on the fundamental frequency of the grid. Other advanced methods for frequency adaptive quadrature-signals generation have been reported in the literature, e.g., the *Hilbert* transformation-based PLL (HT-PLL) [10] or the inverse *Park* transformation-based PLL (IPT-PLL) [11], however they become also complex. With the aim of simplifying, this work proposes the use of a second order generalized integrator (SOGI) [12]-[13] for quadrature-signals generation. The SOGI-QSG scheme is shown in Fig. 2(a) and its characteristic transfer functions are given by :

$$D(s) = \frac{v'}{v}(s) = \frac{k\omega' s}{s^2 + k\omega' s + \omega'^2} \tag{6a}$$

$$Q(s) = \frac{qv'}{v}(s) = \frac{k\omega'^2}{s^2 + k\omega' s + \omega'^2} \tag{6b}$$

where ω' and k set resonance frequency and damping factor of the SOGI-QSG respectively. Bode plots from transfer functions of (6) are shown in Fig. 2(b) and 2(c) for several values of k. These plots show how the lower value of k the more selective filtering response, but the longer stabilization time as well. A critically-damped response is achieved when $k = \sqrt{2}$. This value of gain results an interesting selection in terms of stabilization time and overshot limitation.

If v is a sinusoidal signal with frequency ω, it can be expressed as a phasor $\mathbf{v}$. Therefore the SOGI-QSG outputs can be calculated from (6) as follow:

$$\mathbf{v}' = \mathbf{D}\mathbf{v} \begin{cases} |\mathbf{D}| = \dfrac{k\omega\omega'}{\sqrt{\left(k\omega\omega'\right)^2 + \left(\omega^2 - \omega'^2\right)^2}} \\ \underline{|\mathbf{D}} = \tan^{-1}\left(\dfrac{\omega'^2 - \omega^2}{k\omega\omega'}\right) \end{cases} \tag{7a}$$

$$\mathbf{qv}' = \mathbf{Q}\mathbf{v} \begin{cases} |\mathbf{Q}| = \dfrac{\omega'}{\omega}|\mathbf{D}| \\ \underline{|\mathbf{Q}} = \underline{|\mathbf{D}} - \dfrac{\pi}{2} \end{cases} \tag{7b}$$

It is worth to remark from (7), that qv' is always 90-degrees lag respect to v', independently of the value of k, ω and ω'. This is a very interesting feature for implementing

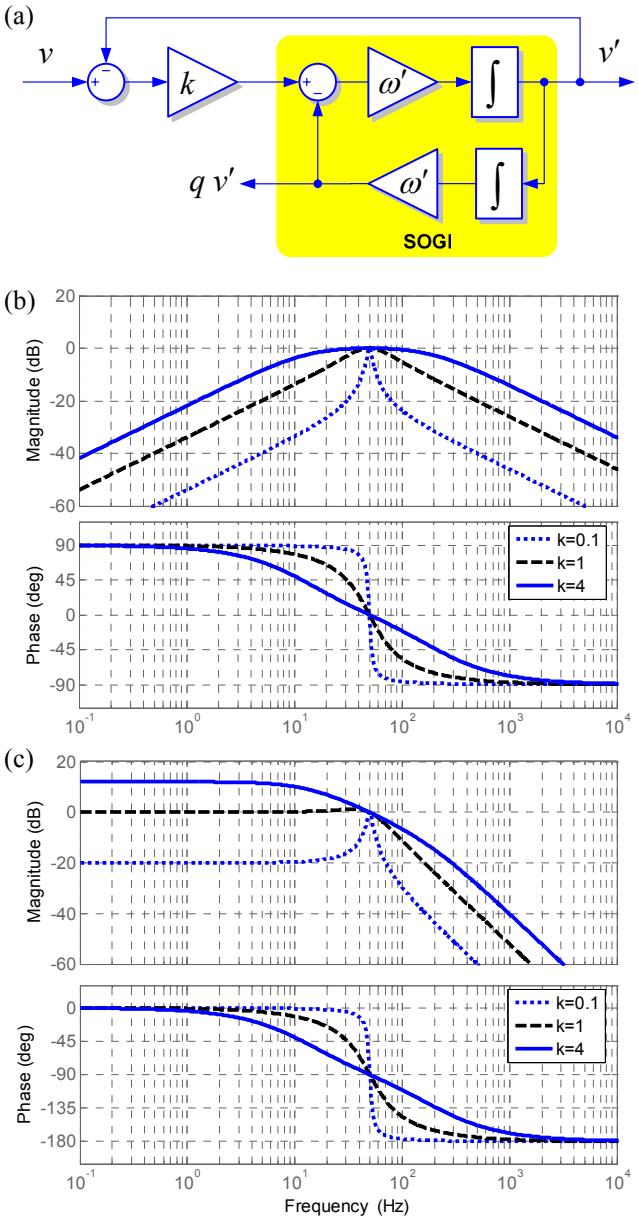

Fig. 2. SOGI-QSG. (a) SOGI-QSG scheme, (b) Bode plot of *D(s)*, (c) Bode plot of *Q(s)*.

the 90-degrees phase-shifting of the q operator. However, (7) also evidences that the SOGI-QSG output signals will be wrong in both amplitude and phase when the SOGI-QSG resonant frequency, ω', does not match up to the input signal frequency, ω. The consequence of these errors will be analyzed in the next section.

IV. POSITIVE-SEQUENCE DETECTOR USING A DUAL SOGI-QSG

The essential structure of the proposed positive-sequence detection system is shown in Fig. 3 where a dual SOGI-QSG (DSOGI-QSG) provides the input signals to the PSC on the $\alpha\beta$ reference frame. To evaluate the response of the system it will be supposed that the grid voltage suddenly experiments a complex voltage sag (dip) type D as a

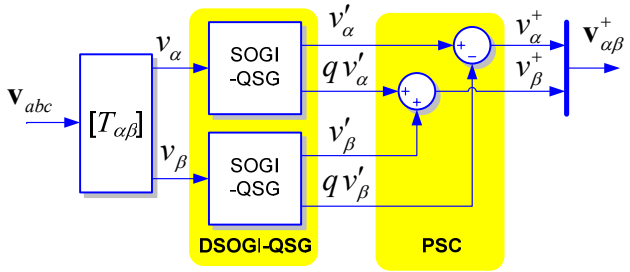

Fig. 3. Positive sequence calculation based on DSOGI-QSG

consequence of a fault condition which is cleared after 100ms [14]. In this dip, the characteristic voltage is $0.6\angle -20^\circ$ and the positive-negative factor is $0.9\angle -10^\circ$, both of them expressed in p.u. respect to the perfectly balanced pre-fault voltage $\mathbf{v}^+_{pf} = 1\angle 0^\circ$. Consequently, the positive and negative sequence fault voltages are given by $\mathbf{v}^+ = 0.747\angle -14^\circ$ and $\mathbf{v}^- = 0.163\angle 8.63^\circ$ respectively. In this simulation, it is assumed that the DSOGI-QSG resonance frequency perfectly matches up with the grid frequency, that is $\omega = \omega' = 2\cdot\pi\cdot 50$ rad/s. In addition, the gain of the DSOGI-QSG has been set at $k = \sqrt{2}$. Fig. 4 shows the response of the PSC under such operating conditions when the DSOGI-QSG is perfectly synchronized. The faulty phase-voltages are shown in Fig. 4(a) and the estimated positive-sequence phase-voltages in the natural *abc* reference frame are shown in Fig. 4(e).

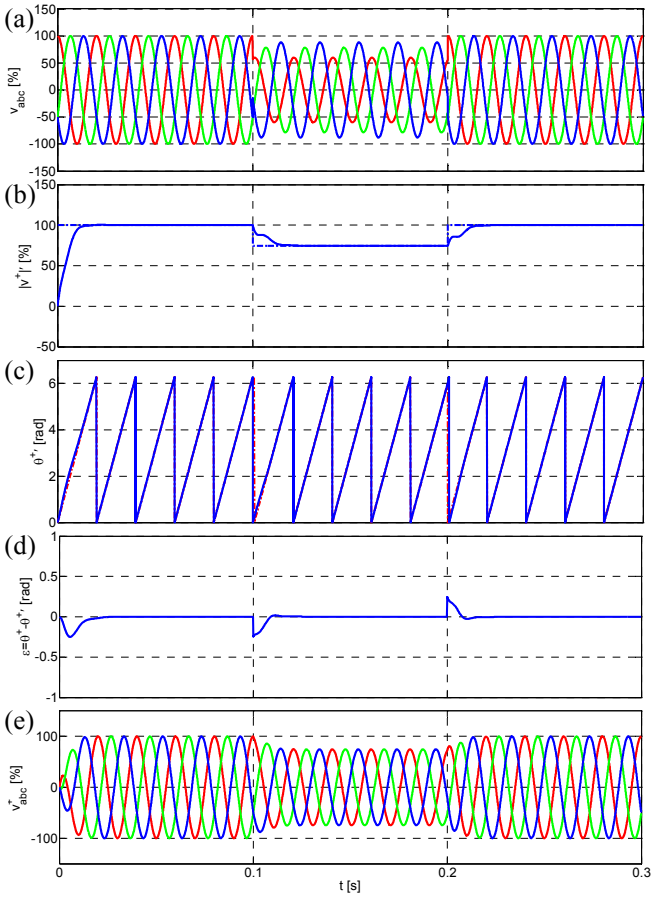

Fig. 4. Response of the PSC in presence of unbalanced voltage sag.

Fig. 4(b) shows the actual and estimated amplitude for the positive-sequence component, $\mathbf{v}^+$, whereas its actual and estimated phase angle are shown in Fig. 4(c). These waveforms are calculated as follows:

$$\left|\mathbf{v}^+\right|' = \sqrt{\left(v^+_\alpha\right)^2 + \left(v^+_\beta\right)^2} \quad ; \quad \theta^{+\prime} = \tan^{-1}\frac{v^+_\beta}{v^+_\alpha}. \tag{8}$$

Fig. 4(d) shows the error in phase-angle estimation. Plots of Fig. 4 confirm the good behavior of the proposed system, which is canceling the steady-state error after one cycle of the grid voltage.

As studied in Section III, when the grid frequency differs from the DSOGI-QSG resonance frequency, the input signals to the PSC show amplitude and phase errors. Nevertheless such signals are always orthogonal. This last characteristic makes easy to analyze how DSOGI-QSG errors are propagated through the PSC. Expressing the n^{th} harmonic of v_α as the phasor $\mathbf{v}^n_\alpha$, it can be concluded from (3) and (7) that the output of the PSC is given by:

$$\mathbf{v}^+_\alpha = \mathbf{P}^n\mathbf{v}^n_\alpha \begin{cases} \left|\mathbf{P}^n\right| = \dfrac{k\omega'}{2}\sqrt{\dfrac{\left(n\omega+\omega'\right)^2}{\left(kn\omega\omega'\right)^2 + \left(n^2\omega^2 - \omega'^2\right)^2}} \\ \angle\mathbf{P}^n = \operatorname{sgn}(n)\tan^{-1}\left(\dfrac{\omega'^2 - n^2\omega^2}{kn\omega\omega'}\right) \\ \qquad -\dfrac{\pi}{2}\left(1-\operatorname{sgn}\left(n^2\omega + n\omega'\right)\right) \end{cases}, \tag{9a}$$

$$\left|\mathbf{v}^+_\beta\right| = \left|\mathbf{v}^+_\alpha\right| \quad ; \quad \angle\mathbf{v}^+_\beta = \angle\mathbf{v}^+_\alpha - \operatorname{sgn}(n)\frac{\pi}{2}, \tag{9b}$$

where ω is the fundamental grid frequency, ω' is the DSOGI-QSG resonance frequency, and positive –negative sign of n represents positive –negative-sequence of the input voltage. Magnitude calculation of (9a) is plotted in Fig. 5 for $k = \sqrt{2}$. This plot evidences that the system of Fig. 3 acts as both a low-pass filter for positive-sequence and a notch filter for negative-sequence. Another remarkable aspect in this plot is the high-order harmonics attenuation, which is a very convenient feature to make the detection technique more robust in front of grid voltage distortion. Expressions of (9) accurately quantify the error in the positive-sequence calculation when the DSOGI-QSG

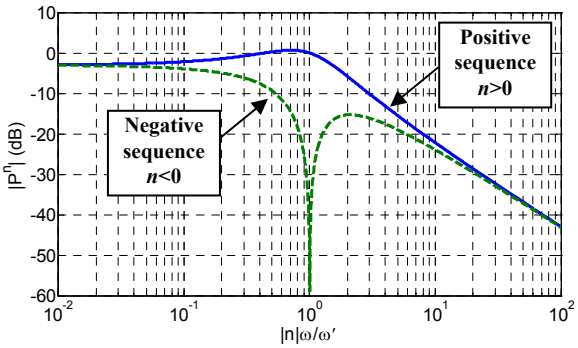

Fig. 5. Frequency response of the PSC based on DSOGI-QSG

resonance frequency does not match up with the grid frequency. These equations can be used to compensate the estimation error when the actual grid frequency is properly detected by an additional mechanism such as a PLL. In this work, although a PLL is employed for grid frequency detection, its output is not used to calculate and compensate the error of (9). In this case however, the output of the PLL dynamically modifies the resonance frequency of the DSOGI-QSG in order to achieve the frequency-adaptive functionality in the proposed positive-sequence detector.

V. POSITIVE-SEQUENCE DETECTOR USING A FREQUENCY-ADAPTIVE DSOGI

To ensure that the proposed positive-sequence detector gives rise to precise results under grid frequency variations it is necessary to implement some kind of close-loop system which allows proper adaptation of the DSOGI-QSG resonance frequency to the actual network conditions. One way to achieve this is by using a single-phase EPLL, HT-PLL, or IPT-PLL on v_α^+–or v_β^+–to detect the grid frequency and dynamically modify the DSOGI-QSG resonance frequency. The EPLL brings to the simplest single-phase implementation among previous three options. However the EPLL is not employed in this work because its filtering characteristic provides the same functionality as the SOGI-QSG. Although the joint action of both filtering stages improves the steady state response of the detection system in presence of high levels of voltage distortion, it also increases output oscillations and extends the stabilization period when the grid experiments voltage sags.

In the proposed system, the well known SRF-PLL structure is used instead of the single-phase PLL for grid frequency detection and subsequent DSOGI-QSG resonance frequency adaptation. The structure of this DSOGI-based PLL (DSOGI-PLL) is presented in Fig. 7, where the positive-sequence voltage vector is translated from the $\alpha\beta$ stationary reference frame to the dq rotating reference frame by means of *Park*'s transformation, that is:

$$\mathbf{v}_{dq}^{+} = \begin{bmatrix} v_d^+ \\ v_q^+ \end{bmatrix} = \left[T_{dq}\right]\mathbf{v}_{\alpha\beta}^{+} \quad ; \quad \left[T_{dq}\right] = \begin{bmatrix} \cos\theta^+ & \sin\theta^+ \\ -\sin\theta^+ & \cos\theta^+ \end{bmatrix}. \quad (10)$$

In the system of Fig. 7, the feedback loop regulating the q component to zero is controlling the angular position of the dq reference frame and estimating the grid frequency.

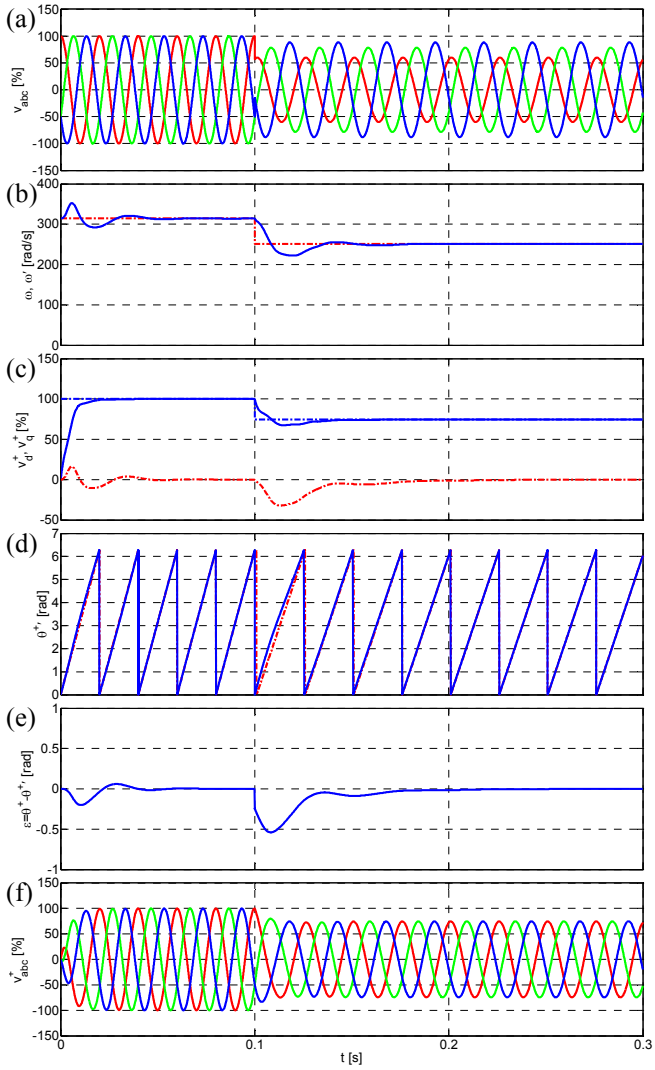

Fig. 6: Characteristic signals of the DSOGI-PLL under a frequency step (50Hz to 40Hz) with k=1.41, k_p=2.22, and k_i=61.69.

The estimated grid frequency, ω', is used by the outer feedback loop to dynamically adapt the DSOGI-QSG resonant frequency.

Fig. 6 shows the DSOGI-PLL response when the grid frequency hypothetically changes from 50 Hz to 40 Hz during an unbalanced sag. Parameters of the SRF-PLL PI controller were calculated according to [5], i.e., k_p=2.22 and k_i=61.69 which implies that cut-off frequency and damping factor are $\omega_c = 2\pi \cdot 12.5$ and $\xi = \sqrt{2}$, respectively.

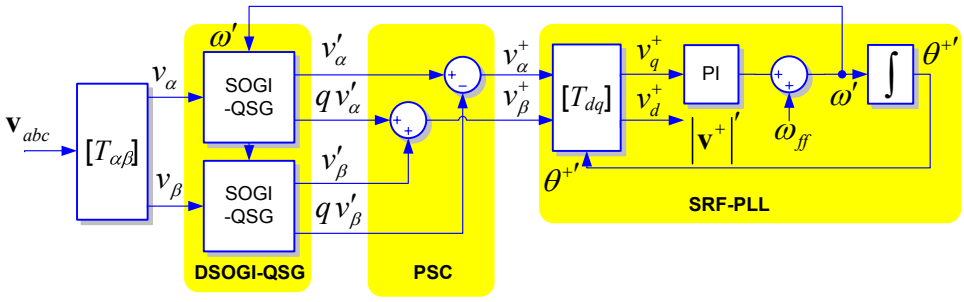

Fig. 7. Block diagram of the DSOGI-PLL

Fig. 6(b) shows the grid frequency step (-20%) and how the SRF-PLL evolutions toward the new frequency value. It is worth to remark that, in front of this big frequency jump, the response of the positive-sequence detector is in steady state again after a stabilization period shorter than 100 ms.

To evaluate the effect of the SRF-PLL on the dynamics of the detection system, the faulty voltages used in Section IV are now applied to the input of the DSOGI-PLL of Fig. 7. The most significant signals from this simulation are shown in Fig. 8, where it is possible to observe the good behavior of the proposed frequency-adaptive positive-sequence detector. Regarding simulation results shown in Fig. 4, the additional delay due to the SRF-PLL is small and the response of the system is completely stabilized after about two grid cycles.

The robustness of the DSOGI-PLL in presence of distorted grid voltages is finally evaluated. In this simulation, the unbalanced and distorted grid voltage during the fault consisted of $\mathbf{v}^{+1} = 0.747\angle -14^\circ$, $\mathbf{v}^{-1} = 0.163\angle 8.63^\circ$, $\mathbf{v}^{-5} = 0.07\angle -60^\circ$ and $\mathbf{v}^{+7} = 0.05\angle 30^\circ$, being $\mathbf{v}_{pf}^{+1} = 1\angle 0^\circ$ the pre-fault grid voltage. Fig. 9 illustrates the behavior of the DSOGI-PLL in such operating conditions and verifies its harmonics rejection capability. Positive-sequence voltage of Fig. 9(e) is practically sinusoidal and balanced, and its harmonic components are given by $\mathbf{P}^{-5}\mathbf{v}^{-5} = 0.008\angle -113^\circ$ and $\mathbf{P}^{+7}\mathbf{v}^{+7} = 0.0057\angle -48^\circ$.

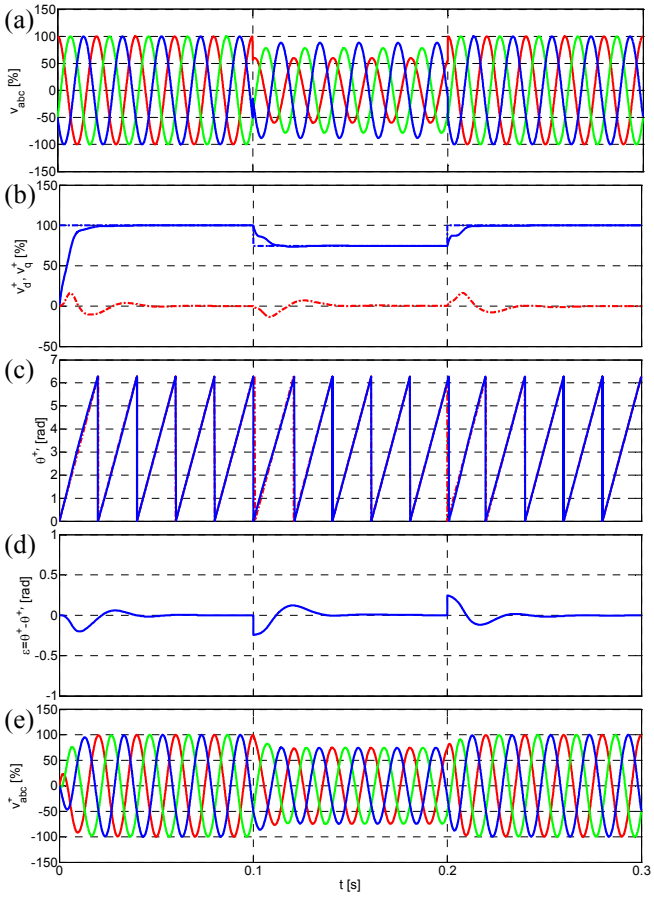

Fig. 8: Characteristic signals of the DSOGI-PLL in presence of an unbalanced voltage sag with k=1.41, k_p=2.22, and k_i=61.69.

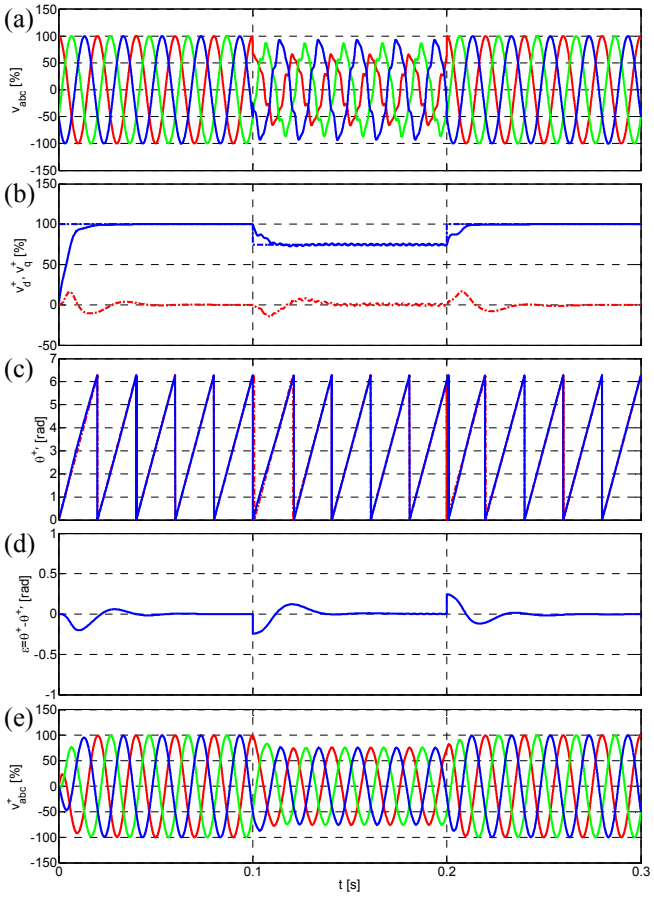

Fig. 9: Characteristic signals of the DSOGI-PLL in presence of distorted and unbalanced grid voltages with k=1.41, k_p=2.22, and k_i=61.69.

VI. CONCLUSION

From the study and results presented in this paper, it can be concluded that the proposed DSOGI-PLL provides an effective solution for grid synchronization of power converters under grid faulty conditions.

The DSOGI-PLL is based on a systematic use of well known techniques. The SOGI is the building block of the QSG and offers harmonic blocking capability to the system. The ISC method on the $\alpha\beta$ reference frame provides an effective mechanism to easily calculate the positive-sequence voltage component. The SRF-PLL makes the detection system frequency-adaptive. The joint action of such techniques converts the DSOGI-PLL to a high-performance detection system which allows fast and precise characterization of the positive-sequence voltage component even under extreme unbalanced and distorted grid operating conditions. Conclusions drawn from the theoretical study of the DSOGI-PLL are ratified by simulation.

ACKNOWLEDGMENT

This work was supported by Ministerio de Ciencia y Tecnologia of Spain under Project ENE2004-07881-C03-02.

REFERENCES

[1] C. Jauch, J. Matevosyan, T. Ackermann, and S. Bolik, "International comparison of requirements for connection of wind turbines to power systems," *Wind Energy*, vol. 8, pp. 295-306, Jul. 2005.

[2] A. Ghosh and A. Joshi, "A new algorithm for the generation of reference voltages of a DVR using the method of instantaneous symmetrical components," *IEEE Power Eng. Review*, vol. 22, pp. 63-65, Jan. 2002.

[3] T. Ackermann, *Wind Power in Power Systems*, England: John Wiley & Sons, Ltd., 2005.

[4] V. Kaura and V. Blasco, "Operation of a phase locked loop system under distorted utility conditions," *IEEE Trans. Ind. Applicat.*, vol. 33, pp. 58-63, Jan./Feb. 1997.

[5] S. Chung, "A phase tracking system for three phase utility interface inverters," *IEEE Trans. Power Electron.*, vol. 15, pp. 431-438, May 2000.

[6] P. Rodríguez, J. Pou, J. Bergas, I. Candela, R. Burgos, and D. Boroyevich, "Double synchronous reference frame PLL for power converters," *in Proc. IEEE Power Electron. Spec. Conf. (PESC'05)*, 2005, pp. 1415-1421.

[7] M. Karimi-Ghartemani and M.R. Iravani, "A method for synchronization of power electronic converters in polluted and variable-frequency environments," *IEEE Trans. Power Systems*, vol. 19, pp. 1263-1270, Aug. 2004.

[8] W. V. Lyon, *Application of the Method of Symmetrical Components*, New York: McGraw-Hill, 1937.

[9] S. Luo and Z. Hou, "An adaptive detecting method for harmonic and reactive currents," *IEEE Trans. on Ind. Electron.*, vol. 42, pp. 85-89, Feb. 1995.

[10] M. Saitou, N. Matsui, and T. Shimizu, "A control strategy of single-phase active filter using a novel d-q transformation," *in Proc. IEEE Ind. Applicat. Conf. (IAS'03)*, 2003, vol. 2, pp. 1222-1227.

[11] S.M. Silva, B.M. Lopes, B.J.C. Filho, R.P. Campana, and W.C. Bosventura, "Performance evaluation of PLL algorithms for single-phase grid-connected systems," *in Proc. IEEE Ind. Applicat. Conf. (IAS'04)*, 2004, vol. 4, pp. 2259-2263.

[12] X. Yuan, W. Merk, H. Stemmler, J. Allmeling, "Stationary-frame generalized integrators for current control of active power filters with zero steady-state error for current harmonics of concern under unbalanced and distorted operating conditions," *IEEE Trans. on Ind Applicat.*, vol. 38, pp.523 – 532, Mar./Apr. 2002.

[13] R. Teodorescu, F. Blaabjerg, U. Borup, and M. Liserre, "A new control structure for grid-connected LCL PV inverters with zero steady-state error and selective harmonic compensation," *in Proc. IEEE App. Power Electron. Conf. and Exp. (APEC'04)*, 2004, vol.1, pp. 580-586.

[14] L.D. Zhang, M.H.J. Bollen, "Characteristic of voltage dips (sags) in power systems," *IEEE Trans. Power delivery*, vol. 15, pp. 827-832, Apr. 2000.